Bonding modes and electronic properties of single-crystalline silicon nanotubes

Binghai Yan, Gang Zhou, Jian Wu, Wenhui Duan,* and Bing-Lin Gu
Center for Advanced Study and Department of Physics, Tsinghua University, Beijing 100084, People's Republic of China
(Received 3 November 2005; revised manuscript received 30 March 2006; published 26 April 2006)

The structural characteristics, bonding modes, and electronic properties of single-crystalline silicon nanotubes (sc-SiNTs) are investigated by using the first-principles method. These pristine sc-SiNTs with sp^3 hybridization, constructed by the bulklike tetrahedrally coordinated Si atoms, are found to be energetically stable. The electronic property is sensitive to the external diameter, tube-wall thickness, and tube-axis orientation due to quantum confinement effects. A direct band gap is observed in SiNTs with smaller sizes. The band gap increases monotonically with decreasing tube-wall thickness, in accord with the substantial blueshift observed in the experiment. It is suggested that this type of SiNTs would have promising practical applications in nanoscale light-emitting devices and electronic devices.

DOI: 10.1103/PhysRevB.73.155432 PACS number(s): 73.22.−f, 71.15.Mb, 73.21.Hb

I. INTRODUCTION

One-dimensional (1D) silicon (Si) nanostructures have been attracting much attention because of their ideal interface compatibility with conventional Si-based technology[1] and potential applications in nanoscale electronics[2] and optoelectronics.[3] Canham first observed with the naked eye that porous Si can emit efficient visible photoluminescence at room temperature.[4] Successively, single-crystalline Si nanowires (sc-SiNWs) with diameters as small as 1 nm and lengths of a few hundred microns have been fabricated.[5] The photoluminescence and spectroscopy measurements showed that a substantial blueshift[6] as well as a significant increase in the energy gap[7] spontaneously emerges with decreasing size of SiNWs, which are attributed mostly to quantum confinement effects. The functionalized SiNWs were utilized as highly sensitive biological and chemical nanosensors and powerful building blocks for nanoelectronic devices such as field effect transistors due to their fascinating electronic and/or optical properties.[2] In contrast to extensive studies on SiNWs, the research on Si nanotubes (SiNTs) is still in the primary stage. Theoretically, various atomic configurations of SiNTs were assumed, and the structural stabilities and electronic properties were evaluated by diverse calculational approaches.[8–10] Recently, polycrystalline (pc) SiNTs (Ref. 11) and Si microtubes[12] were successfully synthesized. And, the photoluminescence spectra analysis demonstrated that quantum confinement in pc-SiNTs significantly influences and even dominates their photoelectric properties (e.g., the substantial blueshift appears with decreasing thickness of the wall).[11] Except for the fascinating photoelectric and electronic properties like SiNWs, SiNTs also have great potential in fabrications of nanoscale heterostructures owing to their considerable hollow cavities. A typical example is a crystalline SiNT filled with amorphous silica to form a perfect 1D heterostructure.[13]

In principle, sc-Si, rather than pc-Si, is more suitable and efficient for practical applications in electronics and photoelectronics, because of the high carrier mobility and pristine structure. More recently, owing to the successful fabrication of self-assembled crystal [111] SiNTs on silicon monoxide,[14] much experimental effort has been devoted to searching for sc-SiNTs, which is expected to be more useful in the development of novel 1D nanoscale devices. Therefore, in this paper, following the experimental observations,[11,14] we artificially construct SiNTs from bulk crystalline Si, and evaluate their stabilities and study their structural characteristics, bonding modes, and electronic properties by using the first-principles method. We will reveal the correlation between the structure and electronic property of sc-SiNTs, clarifying quantum size effects. Furthermore, we thoroughly explore the possibility of "direct" band gap and the size-induced transition from "indirect" to "direct" band gap in these sc-SiNTs. Finally, we speculate on the prospects of this type of Si tube in future nanoscale visual light-emitting devices and electronic devices.

II. CALCULATIONAL MODEL AND METHOD

Based on the recognized experimental achievements,[11,14] in this work sc-SiNTs are constructed from bulk crystalline (cubic diamond) Si along the low-indexed directions [100], [110], and [111], and the atomic configurations are analogous to the counterpart SiNWs with a hollow cavity inside (Fig. 1). In order to eliminate the surface states from the gap, H termination is adopted to passivate all Si dangling bonds on the surfaces. Our calculations are implemented by using the SIESTA code[15] within the framework of density functional theory (DFT). It is known that different basis sets used in the calculation may lead to some difference in calculated results. We have performed some test calculations with the double-

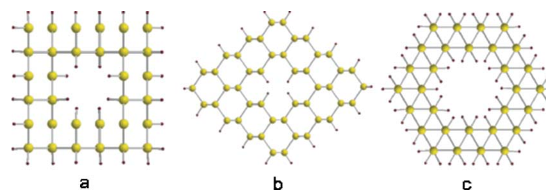

FIG. 1. (Color online) Atomic configurations of sc-SiNTs along (a) [100], (b) [110], and (c) [111] orientations viewed from the top. Filled yellow and gray, and brown and black circles stand for Si and H atoms, respectively.

 ©2006 The American Physical Society

zeta polarized (DZP) and single-zeta polarized (SZP) numerical atomic orbitals basis sets. Although the band structure obtained is slightly different for two different basis sets (e.g., for the [111] sc-SiNT with the external diameter of 1.80 nm and the thickness of 0.63 nm, the calculated band gap is 2.65 eV for DZP and 2.59 eV for SZP), the basic characteristics are the same. Therefore, the SZP numerical atomic orbitals basis set is adopted in the following electronic structure calculations. The core electrons are represented by the standard norm-conserving Troullier-Martins pseudopotentials,[16] and the local density approximation proposed by Perdew and Wang[17] is used for the exchange-correlation energy. Periodic boundary condition is employed in the x-y plane with at least 10 Å separation between the two closest H atoms on neighboring tubes. The cutoff of grid integration of charge density is set to 100 Ry and 2–10 k points along the tube axis are used. Structural optimizations are performed using conjugate gradient method and deemed sufficiently converged when the residual forces on all ions are smaller than 0.04 eV/Å. It is known that DFT underestimates the band gaps of semiconductors and insulators.[18] Thus, by comparing the calculated band gap with experimental value of bulk crystalline Si, we present an upshift of 0.46 eV for the conduction bands of sc-SiNTs as the self-energy correction in the following calculations. Then, we calculate the band structures of SiNWs along [100] orientation with diameters ranging from 0.5 to 2.3 nm, and confirm that the obtained band gaps are in good agreement with the previous results by other calculational models.[19,20] This indicates that the parameters adopted in our calculations are suitable.

III. RESULTS AND DISCUSSION

From the optimized geometry, we find that stable sc-SiNTs in substance inherit the structural characteristics of bulk crystalline Si. The coordination number of every Si atom in the tube is four. The calculated bond length and bond angle are, respectively, 2.37 ± 0.01 Å and $109\pm2°$, which are close to the ideal single Si-Si bond length of 2.35 Å and the angle between the two standard sp^3 hybridization bonds of 109.5°. The composition analysis on the overall local density of states of every Si atom shows an efficient mixing of p_x, p_y, p_z, and s atomic orbitals. In all resulting valence and conduction bands, there is no clear separation of delocalized π bonding and the localized σ bonding formed by the sp^2 hybrid orbitals. In brief, all of the information on the bonding reveals that chemical bonds in sc-SiNTs are compatible with rigid sp^3 hybridization, which is in accord with the fact that Si prefers sp^3 bonds rather than sp^2 bonds.[21] Moreover, our calculated binding energy (per Si atom) of sc-SiNTs is 0.5 eV larger than those of hypothetical thinnest single-walled SiNTs (SW-SiNTs) introduced by Bai *et al.*[8] (Note: in such SW-SiNTs, all Si atoms are fourfold coordinated but the bond angles can be quite different from 109°.) From the general bonding characteristics of Si and the essential requirements of the direction and saturation of covalent bonds, it can be concluded that the pristine nanotube constructed by the bulklike tetrahedrally coordinated Si atoms is likely to be a more stable atomic configuration of 1D Si nanostructures than the hypothetical rolled-up graphitelike sheet and the cluster-assembled configurations.[8–10] This assertion also agrees with the simulation results by Zhang *et al.*[10] that the rolled-up graphitelike sheet tubular structure for Si is less stable and tends to relax to the diamondlike structure for the largest extent of overlap of sp^3 hybridized orbitals.

By *ab initio* calculations, Bai *et al.* have predicted that SW-SiNTs with diameters from 8.98 to 10.65 Å are locally stable in vacuum at zero temperature and exhibit metallic behavior.[8] In comparison with SW-SiNTs, sc-SiNTs introduced here have larger sizes and more compact structures, and more complicated quantum confinement behaviors. In principle, sc-SiNTs can be well-defined by the external diameter D, the tube wall thickness σ, and the orientation of the tube axis $[uvw]$. To the best of our knowledge, quantum confinement effects in any crystalline nanotubes have not been systematically investigated and are not clearly addressed to date. What are the main structural parameters determining the electronic properties, and how do they influence the electronic properties or confine the electrons' propagations along the circumferential and radial directions? In what follows, we will thoroughly explore quantum confinement effects in sc-SiNTs from the geometry and size.

As predicted for sc-SiNWs,[22] a direct band gap is observed in sc-SiNTs as their sizes are reduced to certain nanoscale values. But, compared with counterpart sc-SiNWs, the critical external diameter (corresponding to the appearance of the direct band gap) of sc-SiNTs will be somewhat larger due to their hollow cavities. Typically, the band gaps of [111] SiNWs are indirect when $D\geqslant1.80$ nm, while sc-SiNTs with $D=1.80$ nm remain direct at Γ and become indirect when D increases appreciably (Fig. 2). Furthermore, [110] sc-SiNTs are also found to have a direct gap at Γ when $D\leqslant2.58$ nm, and become indirect as D increases to 2.97 nm. However, [100] sc-SiNTs exhibit a direct band gap at Γ for all the external diameters investigated (from 1.19 to 2.97 nm). It is found that during the transition from "direct to indirect" band gap, the valence-band maximum (VBM) of SiNTs is at the zone center (i.e., Γ point) all along; in contrast, the position of the conduction-band minimum (CBM) shifts from Γ to the non-zone-center point, as shown in Figs. 2(a) and 2(b). The size effect on electronic structure can be illustrated visually by the wave function of the CBM. Qualitatively, the wave functions of the CBMs in [111] SiNTs with the direct band gap (i.e., $D\leqslant1.80$ nm) are characterized as high symmetry and are uniformly delocalized at all sites [Fig. 3(a)], whereas those with the indirect band gap (i.e., $D>1.80$ nm) have low symmetry and are only randomly localized at some special sites [Fig. 3(b)]. These phenomena are attributed to quantum confinement effects along the circumferential direction: the folded transverse and longitudinal valleys of Si tubes have significantly different effective masses in the lateral direction, and the difference determines the order of CBMs and results in the presence of an indirect or direct band gap. Meanwhile, Fig. 2 evidently shows that, for the tubes with the fixed external diameter, the band gap increases with decreasing tube-wall thickness, but the band gap character (i.e., direct or indirect) is unchanged, which can also be reflected by the similarity of wave func-

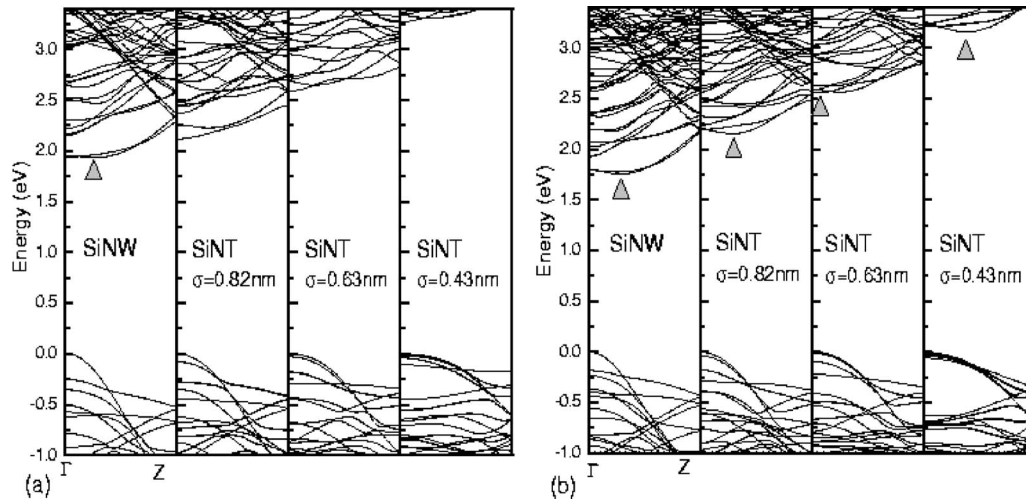

FIG. 2. Band structures of sc-SiNTs and sc-SiNWs along [111] orientation with different external diameters D and tube-wall thicknesses σ (only for sc-SiNTs): (a) $D=1.80$ nm; (b) $D=2.19$ nm. The indirect conduction-band minima (not at Γ) are indicated by the triangles.

tions of CBMs. Importantly, the feature that the CBM of sc-SiNTs is only sensitive to the external diameter and insensitive to the tube-wall thickness indicates that the direct band gap emerging would be substantial. This information would be crucial for highly efficient applications of SiNTs in optoelectronics, such as light-emitting devices with extremely low power consumption.

The electronic properties of sc-SiNTs oriented along three low-index directions with respect to the external diameter and tube-wall thickness are also studied quantitatively. In Fig. 4, the variations of band gaps of sc-SiNTs with the tube-wall thickness are illustrated to clarify quantum confinement effects along the radial direction more distinctly. Typically, the band gaps of these Si tubes increase monotonically and significantly as the tube-wall thickness decreases, which is in accord with the experimental observation of a blueshift of photoluminescence peak caused by the thickness decrease of the SiNT wall.[11] All sc-SiNTs along one certain orientation with the same thickness have almost the identical band gap, no matter what their external diameters are, except for the thinnest ones (marked by circles in Fig. 4) with largest stress-induced deformation. Similar behavior has not been

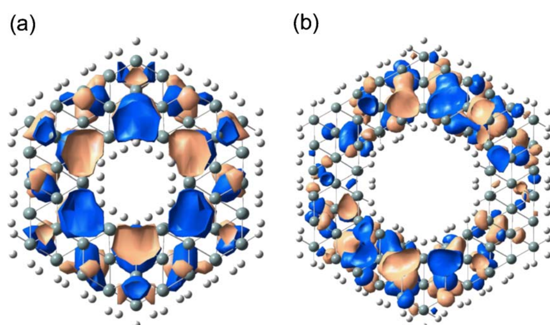

FIG. 3. (Color online) Wave functions of conduction band minima at Γ of sc-SiNTs along [111] orientation with different external diameters: (a) $D=1.80$ nm (direct band gap); (b) $D=2.19$ nm (indirect band gap). Blue and dark gray, and brown and light gray regions + and −, respectively.

observed in multiwalled carbon nanotubes and sc-SiNWs. These characteristics can be semiquantitatively interpreted by a "particle in an infinite tubular potential well" model with the external diameter D and the well width σ. The stationary solutions of this model can be obtained as $\psi_{nl}(r,\phi)=[AJ_l(k_{nl}r)+BY_l(k_{nl}r)]e^{il\phi}$, where $l=0,1,2,\ldots$, $J_l(kr)$ and $Y_l(kr)$ are the first and second kind of Bessel functions with A and B as their coefficients, respectively, and k_{nl} is the nth solution of the equation

$$\begin{vmatrix} J_l(k_{nl}r_0) & Y_l(k_{nl}r_0) \\ J_l(k_{nl}(r_0-\sigma) & Y_l(k_{nl}(r_0-\sigma)) \end{vmatrix} = 0,$$

which is derived from the boundary conditions

$$\begin{cases} \psi_{nl}(r_0) = 0, \\ \psi_{nl}(r_0-\sigma) = 0, \end{cases}$$

with $r_0=D/2$. The eigenvalues are $E_{nl}=\hbar^2k_{nl}^2/2m^*$, where m^* is the effective mass. The numerical solutions can be easily calculated. In this simple single-electron model, the two lowest energy levels correspond to the ground state and the first excited state, respectively. So, the difference (ΔE) between them can be approximately or semiquantitatively treated as the counterpart of the band gap of the real electronic structure due to similar quantum confinement conditions. Figure 4(d) and its inset show the obtained dependence of ΔE on the external diameter D and tube-wall thickness (i.e., well width) σ. For the well with fixed D, ΔE is found to increase dramatically as σ decreases. On the other hand, for the well with fixed σ, ΔE remains almost the same while D varies greatly. These results are in good agreement with our first-principles calculations, as shown in Fig. 4. Interestingly, the characteristics of the electronic structures of SiNTs could be illustrated in a band-by-band fashion. As an example, for the [111] nanotube with $D=1.80$ nm and $\sigma=0.43$ nm, the charge density is plotted in the x-y plane after averaging along the tube axis or z direction. It can be seen that the lowest nine bands [Figs. 5(a)–5(i)] from the above analytic model agree well with the charge density distributions of the lowest nine

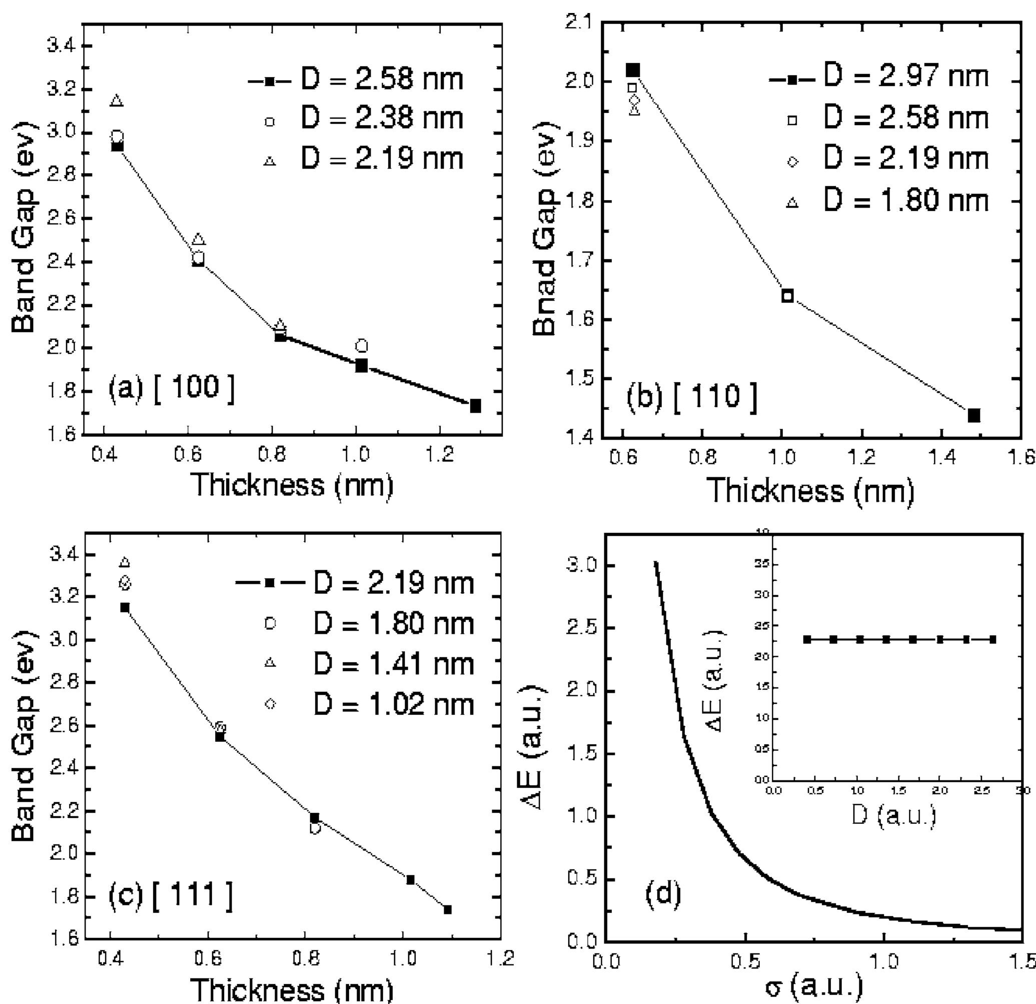

FIG. 4. Dependence of band gap on the tube-wall thickness σ for sc-SiNTs with different external diameters D and orientations: (a) [100], (b) [110], and (c) [111]. The points corresponding to the largest external radius are connected by lines. (d) The simulated energy level difference ΔE with a "particles in an infinite tubular potential well" model vs the well width σ with the fixed external diameter D. The inset is ΔE vs D with the fixed σ.

occupied bands [Figs. 5(1)–(9)] from the first-principles method, which indicates the validity of the particles in an infinite tubular potential well model in this issue. However, such correspondence to the potential well model turns less precise for the higher bands near the Fermi level [Figs. 5(208)–(211)].

It is a unique feature of 1D crystalline nanostructures that the effect of quantum confinement on electronic structure (especially the band gap) depends on the orientation. In principle, the dependence on sc-SiNTs is sensitive to the tube-wall thickness σ, and could be quite different from that in sc-SiNWs.[20] In detail, for sc-SiNTs, we have $E_g^{\langle 100\rangle} > E_g^{\langle 111\rangle} > E_g^{\langle 110\rangle}$ when $\sigma > 0.9$ nm, which is just the same as the case of sc-SiNW, while we have $E_g^{\langle 111\rangle} > E_g^{\langle 100\rangle} > E_g^{\langle 110\rangle}$ when $\sigma < 0.9$ nm. It is due to the hollow cavity and atomic structure of sc-SiNTs. For future practical applications of sc-SiNTs in nanoscale devices, it would be worthwhile to determine the critical point between the tube behavior and the wire behavior.

More abundant and complex quantum confinement effects in sc-SiNTs may imply more significant application potential in nanoscale optoelectronics and electronics. The existence of a direct band gap is favorable for the application of sc-SiNTs as highly efficient light-emitting devices. In comparison with counterpart sc-SiNWs, the feature of SiNTs that the band gap is related to the tube-wall thickness is advantageous to the electronic property engineering of synthesized single transistors. The considerable hollow cavity provides a convenient physical channel to tailor the electronic property of sc-SiNTs by doping with guest species. In particular, a 1D nanometer *p-n* junction would be conveniently realized by doping group III or V elements into one pristine sc-SiNT. Furthermore, SiNTs could be an ideal mold for encapsulating materials, and the formed heterostructures might be highly advantageous to open up promising applications in various nanoelectronic devices. High specific surface area, combined with the stable atomic structure, enables sc-SiNTs to be used as nanosensors for detection of biological and chemical species and field-effect transistors for various circumstance, like sc-SiNWs.[2]

Very recently, De Crescenzi *et al.* reported experimental evidence of tubular SiNTs that have an atomic arrangement compatible with a puckered structure and different chirali-

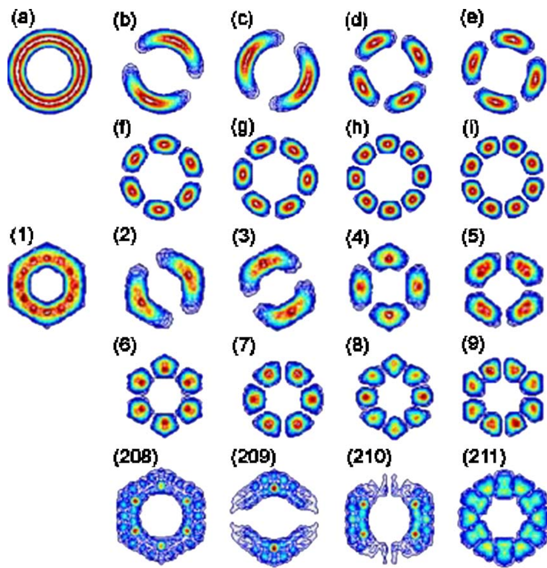

FIG. 5. (Color online) Charge density in the x-y plane (integrated along the tube axis or z direction) for the [111] sc-SiNT of $D=1.80$ nm and $\sigma=0.43$ nm. The band indices (1)–(9) and (208)–(211) are shown for each figure. The results of a "particles in an infinite tubular potential well" model are shown in the top panels marked with (a)–(i) with respect to bands (1)–(9). The high (low) density region is indicated by red and blue (dark and light gray).

ties. Those chiral SiNTs could exhibit metallic or semiconducting behavior, depending on the chirality,[23] while the sc-SiNTs are constructed by the bulklike tetrahedrally coordinated Si atoms on the basis of previous experimental observations,[11,14] and are semiconducting. Obviously, the chiral SiNTs and the sc-SiNTs studied are quite different in the structural and electronic properties, although the bonding mode is believed to be of sp^3 hybridization in both cases. It would be interesting to theoretically explore the detailed geometry and electronic properties of the chiral SiNTs in the future.

IV. CONCLUSION

In conclusion, following unambiguous experimental observations, we present sc-SiNT, a 1D Si tubular nanostructure, from bulk crystalline Si. Using first-principles calculations, we confirm the stability of sc-SiNT and study the structural characteristics, bonding modes, and electronic properties of sc-SiNTs oriented along [100], [110], and [111] directions. sc-SiNTs maintain the essential structural characteristics of bulk Si: Si atoms in the tubes are all fourfold coordinated and their chemical bonding originates from sp^3 hybridization. In this nanosystem, quantum confinement effects along the circumferential and radial directions are related to three structural parameters: the external diameter of the tube, tube-wall thickness, and tube-axis orientation. In detail, the band-gap character (i.e., direct or indirect) is concerned with the tube external diameter, but is insensitive to the tube-wall thickness. The direct fundamental band gap at Γ is found for [100] sc-SiNTs, while in [110] and [111] sc-SiNTs, the direct band gap is observed in one size range, and the direct to indirect band gap transition occurs when the external diameter increases to one certain size. The band gap increases as the tube-wall thickness decreases and is insensitive to the external diameter. The orientation anisotropy of band gaps of sc-SiNTs is dependent upon the tube-wall thickness. Due to their unique quantum confinement effects and considerable hollow cavities, sc-SiNTs and their derivatives will probably play a key role as interconnects and functional components in future nanoscale electronic and optical devices.

This work was supported by the Natural Science Foundation of China (Grants Nos. 10325415 and 10404016).

*Author to whom correspondence should be addressed. Email address: dwh@phys.tsinghua.edu.cn

[1] Y. Huang, X. Duan, Y. Cui, L. J. Lauhon, K. Kim, and C. M. Lieber, Science **294**, 1313 (2001); L. J. Lauhon, M. S. Gudiksen, D. Wang, and C. M. Lieber, Nature (London) **420**, 57 (2002).
[2] Y. Cui, Q. Q. Wei, H. K. Park, and C. M. Lieber, Science **293**, 1289 (2001); Y. Cui, Z. H. Zhong, D. L. Wang, W. U. Wang, and C. M. Lieber, Nano Lett. **3**, 149 (2003).
[3] M. S. Gudiksen, L. J. Lauhon, J. Wang, D. C. Smith, and C. M. Lieber, Nature (London) **415**, 617 (2002); A. T. Fiory and N. M. Ravindra, J. Electron. Mater. **32**, 1043 (2003).
[4] L. T. Canham, Appl. Phys. Lett. **57**, 1046 (1990).
[5] A. M. Morales and C. M. Lieber, Science **279**, 208 (1998); Y. F. Zhang, Y. H. Tang, N. Wang, D. P. Yu, C. S. Lee, I. Bello, and S. T. Lee, Appl. Phys. Lett. **72**, 1835 (1998); J. D. Holmes, K. P. Johnston, R. C. Doty, and B. A. Korgel, Science **287**, 1471 (2000).
[6] Y. F. Zhang, Y. H. Tang, H. Y. Peng, N. Wang, C. S. Lee, I. Bello, and S. T. Lee, Appl. Phys. Lett. **75**, 1842 (1999).
[7] D. D. D. Ma, C. S. Lee, F. C. K. Au, S. Y. Tong, and S. T. Lee, Science **299**, 1874 (2003).
[8] J. Bai, X. C. Zeng, H. Tanaka, and J. Y. Zeng, Proc. Natl. Acad. Sci. U.S.A. **101**, 2664 (2004).
[9] M. Menon and E. Richter, Phys. Rev. Lett. **83**, 792 (1999).
[10] R. Q. Zhang, S. T. Lee, C. K. Law, W. K. Li, and B. K. Teo, Chem. Phys. Lett. **364**, 251 (2002).
[11] S. Y. Jeong, J. Y. Kim, D. Yang, B. N. Yoon, S. H. Choi, H. K. Kang, C. W. Yang, and Y. H. Lee, Adv. Mater. (Weinheim, Ger.) **15**, 1172 (2003).
[12] J. Hu, Y. Bando, Z. Liu, J. Zhan, and D. Golberg, Adv. Funct. Mater. **14**, 610 (2004).
[13] B. K. Teo, C. P. Li, X. H. Sun, N. B. Wong, and S. T. Lee, Inorg. Chem. **42**, 6723 (2003).
[14] Y. W. Chen, Y. H. Tang, L. Z. Pei, and C. Guo, Adv. Mater. (Weinheim, Ger.) **17**, 564 (2005); Y. H. Tang, L. Z. Pei, Y. W. Chen, and C. Guo, Phys. Rev. Lett. **95**, 116102 (2005).
[15] P. Ordejón, E. Artacho, and J. M. Soler, Phys. Rev. B **53**, R10441

(1996); J. M. Soler, E. Artacho, J. D. Gale, A. Garcia, J. Junquera, P. Ordejón, and D. Sanchéz-Portal, J. Phys.: Condens. Matter **14**, 2745 (2002).
[16] J. P. Perdew and A. Zunger, Phys. Rev. B **23**, 5048 (1981); N. Troullier and J. L. Martins, *ibid.* **43**, 1993 (1991).
[17] J. P. Perdew, Y. Wang, Phys. Rev. B **45**, 13244 (1992).
[18] M. S. Hybertsen and S. G. Louie, Phys. Rev. Lett. **55**, 1418 (1985).
[19] F. Buda, J. Kohanoff, and M. Parrinello, Phys. Rev. Lett. **69**, 1272 (1992); T. Ohno, K. Shiraishi, and T. Ogawa, *ibid.* **69**, 2400 (1992); C. Y. Yeh, S. B. Zhang, and A. Zunger, Phys. Rev. B **50**, 14405 (1994).
[20] C. Delerue, G. Allan, and M. Lannoo, Phys. Rev. B **48**, 11024 (1993).
[21] S. B. Fagan, R. J. Baierle, R. Mota, A. J. R. da Silva, and A. Fazzio, Phys. Rev. B **61**, 9994 (2000).
[22] X. Zhao, C. M. Wei, L. Yang, and M. Y. Chou, Phys. Rev. Lett. **92**, 236805 (2004).
[23] M. De Crescenzi, P. Castrucci, M. Scarselli, M. Diociaiuti, P. S. Chaudhari, C. Balasubramanian, T. M. Bhave, and S. V. Bhoraskar, Appl. Phys. Lett. **86**, 231901 (2005).